Alkaline phosphatase activity assay

The alkaline phosphatase (ALP) activity of cultured cells from 15 samples of noncryopreserved cells (Table 1, nos. 12, 13, and 16–28) and 26 samples of cryopreserved cells (Table 1, nos. 1–6, and 9–28) was examined by the specific conversion of *p*-nitrophenyl phosphate (pNPP) into *p*-nitrophenol (pNP). Reddi and Sullivan have described the method in detail[21]; minor modifications to the method have been described in our previous reports.[22] Briefly, cells scraped into 0.5 mL of ice-cold 10 mM Tris-HCl, 1 mM EDTA, and 100 mM NaCl (pH 7.4) were sonicated and used for measurement of DNA. The DNA contents of the cells were measured with Hoechst 33258 (molecular probe). Twenty microliters of suspended cell solution was added to 0.2 mL of buffer containing Hoechst 33258 (5 μg/mL) and the fluorescence was measured on a microplate reader (Wallac 1420 ARVOsx; PerkinElmer Life and Analytical Sciences, Boston, MA). Standard DNA solutions were prepared with salmon sperm DNA (Invitrogen). After measured DNA contents, sonicated cell solution was centrifuged at 10,000 $\times$ *g* for 1 min at 4°C. An aliquot (20 μL) of the supernatant was assayed for ALP activity, using pNPP solution (Zymed Laboratories, South San Francisco, CA). The cell solutions were incubated at 37°C for 30 min and measured on the microplate reader for absorbance of the pNP product formed at 405 nm. Enzyme activity was expressed as micromoles of pNP produced per 30 min per DNA content. Data represent the mean of at least six independent trials.

Image analysis and calcium assay of extracellular mineralization

Extracellular mineralization by the cells was visualized with calcein, which is a calcium-binding fluorescent chemical used to detect bone minerals. The fluorescence intensity of calcein showed excellent correlations with calcium content.[23,24] Calcein (1 μg/mL) was added to the medium for entire culture periods. The medium containing calcein was removed and cells were washed with PBS immediately before these analyses. The fluorescence of calcein incorporated into extracellular mineral ingredients was visualized and quantified with an image analyzer (Typhoon 8600; 526 nm short-pass filter; Amersham Biosciences, Piscataway, NJ). The scanned fluorescent images were quantitated with ImageQuant TL software (Amersham Biosciences) and represented as intensity per area. We calculated the area under the curve created by a plot of the pixel intensities and the pixel locations along a linear object, such as a line. ImageQuant displays the pixel intensities as a line graph. The results were transferred to Excel (Microsoft, Redmond, WA) and calculated the pixel intensities per selected area. Extracellular mineralization was also observed with a fluorescence microscope (Olympus IX70; Olympus Optical, Tokyo, Japan) as well as a phase-contrast microscope. Data represent the mean of at least six independent experiments.

Statistical data analysis

For statistical analysis of the flow cytometry data, a Kolmogorov–Smirnov (KS) two-sample test was used for the two histograms resulting from gating the following populations[25]: KS statistics calculated by the CellQuest software program (BD Biosciences Immunocytometry Systems) on the whole histograms produced the index of similarity $D/s(n)$ and a D value (Table 2). As for ALP activity per DNA contents and calcium deposition, a two-tailed Student t test computed by JMP 5.0 software (SAS Institute, Cary, NC) was used to determine the statistical significance of the measured differences. Error bars shown in Figs. 3 and 5 indicate the standard deviation (SD). The relationship between cell viability and storage period was displayed in a scatter diagram and the regression line and equation were included in the diagram (Fig. 4).

RESULTS

Human bone marrow cells from 28 patients were cultured to expand mesenchymal cells. The 15 samples of subcultured mesenchymal cells without cryopreservation were maintained for 14 days in osteogenic medium. The degrees of viability of 21 cases of cryopreserved mesenchymal cells were checked immediately after thawing and then subcultured in the same way. Information related to the 28 donors is listed in Table 1.

For analyses of cell surface antigens, both cryopreserved and noncryopreserved cells were negative for hematopoietic stem cell markers CD34, CD45, hematopoietic cell marker CD14, and HLA-DR. However, the cells were strongly positive for CD29 and CD105, all of which are commonly used in the analyses of MSCs. These data coincide well with the reported data of MSC characteristics.[26–32] The analysis also revealed no distinct differences between noncryopreserved and cryopreserved mesenchymal cells (Fig. 1). Furthermore, Kolmogorov–Smirnov (KS) statistics were applied to overlaid histograms between isotype control and each cell surface antibody. This resulted in an index of each pair of curves (Fig. 1), indicating the similarity between noncryopreserved cells and cryopreserved cells ($p < 0.001$) in all cases (Table 2).

To check whether cryopreserved mesenchymal cells have proliferation/osteogenic differentiation capabilities comparable to those of noncryopreserved mesenchymal cells, a 14-day subculture was conducted in the presence or absence of Dex. The expression of ALP changed in a

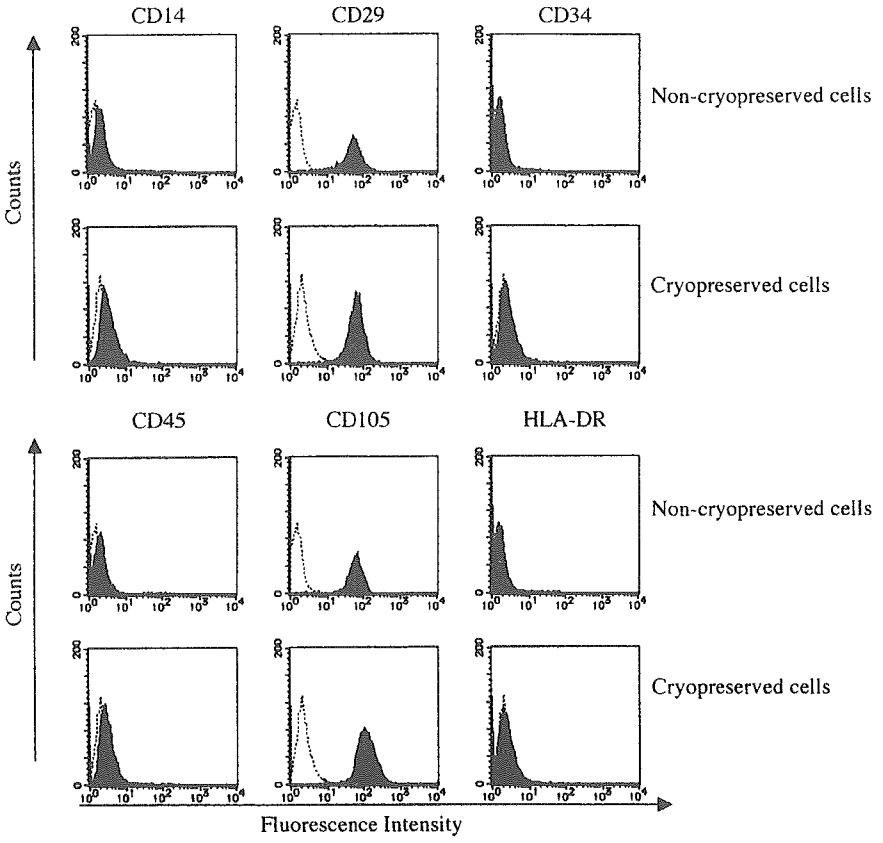

FIG. 1. FACS analyses of noncryopreserved and cryopreserved human mesenchymal cells. Noncryopreserved cells derived from no. 28 and cryopreserved cells derived from no. 9 are represented here. These cells were labeled with FITC-conjugated antibodies against CD14, CD29, CD34, CD45, CD105, HLA-DR, or immunoglobulin G isotype control antibodies. Cells were analyzed with a FACSCalibur. The *x* axis indicates fluorescence intensity (FI). The *y* axis indicates cell counts. Open and solid histograms indicate the results using isotype control immunoglobulin G and specific antibodies, respectively.

TABLE 2. KOLMOGOROV–SMIRNOV TWO-SAMPLE TEST[a]

		KS Two-sample test	
CD marker	*Variable*	*Noncryopreserved cells*	*Cryopreserved cells*
CD14	*D/s(n)*	25.56	26.67
	D	0.42	0.38
CD29	*D/s(n)*	52.82	70.25
	D	0.99	1
CD34	*D/s(n)*	6.71	11.03
	D	0.11	0.16
CD45	*D/s(n)*	19.87	21.45
	D	0.33	0.3
CD105	*D/s(n)*	52.89	69.87
	D	0.99	1
HLA-DR	*D/s(n)*	3.62	3.48
	D	0.06	0.05

[a]The calculation computes the summation of the curves and finds the greatest difference between the summation curves (p 0.001). All indexes of the Kolmogorov–Smirnov two-sample test show the difference between the histogram of CD markers and that of isotype control (see Fig. 1). *D/s(n)*, index of similarity for two curves; *D*, KS statistic (simply, the greatest difference between the two curves). If the indexes of both noncryopreserved cells and cryopreserved cells are close to each other, this means both histograms shown in Fig. 1 are similar to each other.

time-dependent manner and reached a plateau on days 7–11 cultivation. Furthermore, calcium deposition started from day 11 to 14 of cultivation (data not shown). Those time lags were caused by the difference in cell origin, in other words, the condition of the patient. We consequently fixed on day 14 for the analysis because both ALP activity and calcium deposition could be analyzed at one time, even if the plateau in ALP activity was missed by a little.

Calcein enabled us to analyze calcium deposition quantitatively, using an image analyzer (Fig. 2A amd B, panels a), as well as to visualize calcium deposition by fluorescence microscopy (Fig. 2A and B, panels b). The fluorescence intensity of calcein showed excellent correlation with calcium contents as described in Materials and Methods. Furthermore, calcein is easily used in a quantifiable approach to calcium deposition.[23,24] We therefore performed only the calcein assay for calcium deposition. As shown in panels a of Fig. 2, culturing with Dex showed abundant mineralization (calcein uptake) over the entire area of the TCPS as detected with the image analyzer. Mineralization was similarly observed in both noncryopreserved cells (Fig. 2A) and cryopreserved cells (Fig. 2B). Detailed morphology is shown in Fig. 2 by fluorescence and phase-contrast microscopy (panels b and c, respectively). Amorphous mineralized nodular aggregates, seen in panels c of Fig. 2 [Dex(+)], coincided with the fluorescent areas [panels b of Fig. 2, Dex(+)], indicating areas of calcein uptake. When these cells were cultured in the absence of Dex, mineralization was not detected [Fig. 2, Dex(–)]. These patterns of extracellular mineralization were similarly seen in both noncryopreserved and cryopreserved cells.

As shown in Fig. 3, ALP activity and calcein uptake of noncryopreserved mesenchymal cells from 15 cases

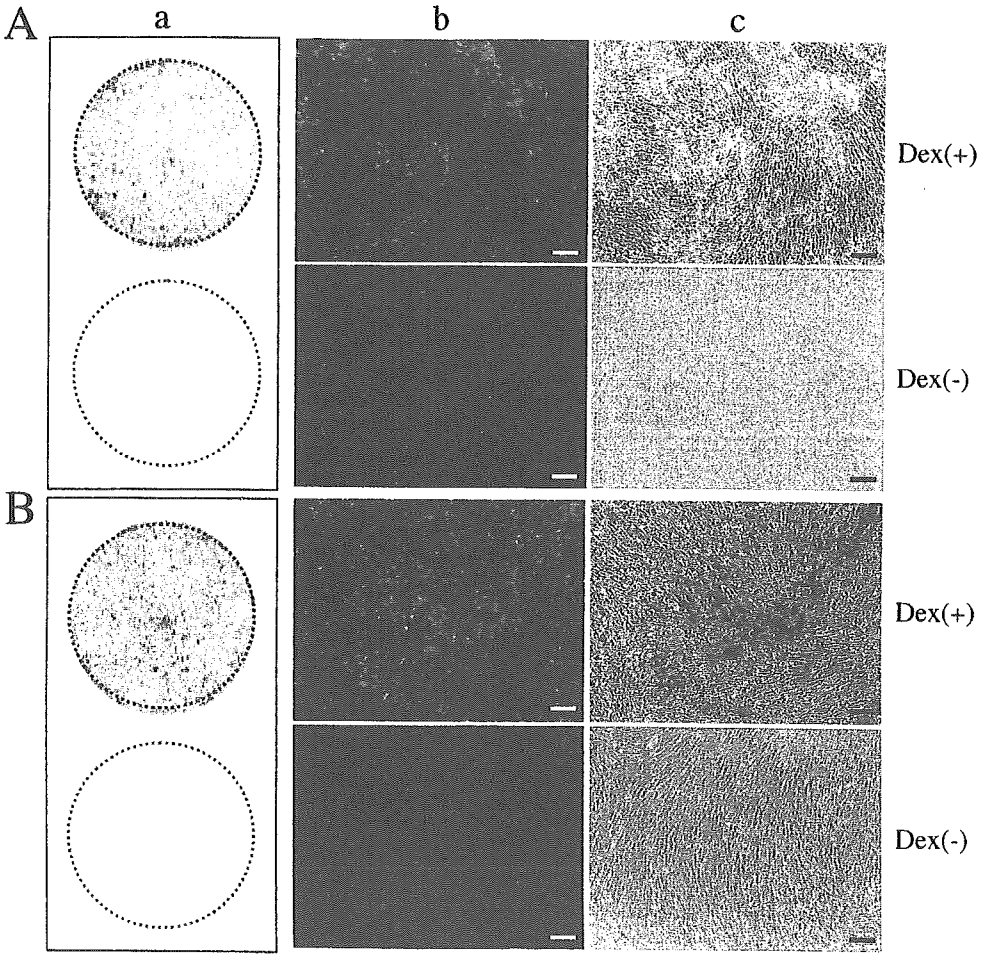

FIG. 2. Cell morphology and mineralization capacity of noncryopreserved and cryopreserved human mesenchymal cells. The noncryopreserved (**A**) and cryopreserved (**B**) cells represented here were derived from sample no. 27. The cells were cultured for 2 weeks in the presence of calcein with (+) or without (−) Dex. Calcium deposition (a) detected by calcein uptake was visualized with an image analyzer. The round area indicates the entire area of the well in 12-well plates. Each micrograph represents a fluorescence image (b) or a phase-contrast image (c). Original magnification: (b and c) ×100. Scale bars: 200 μm.

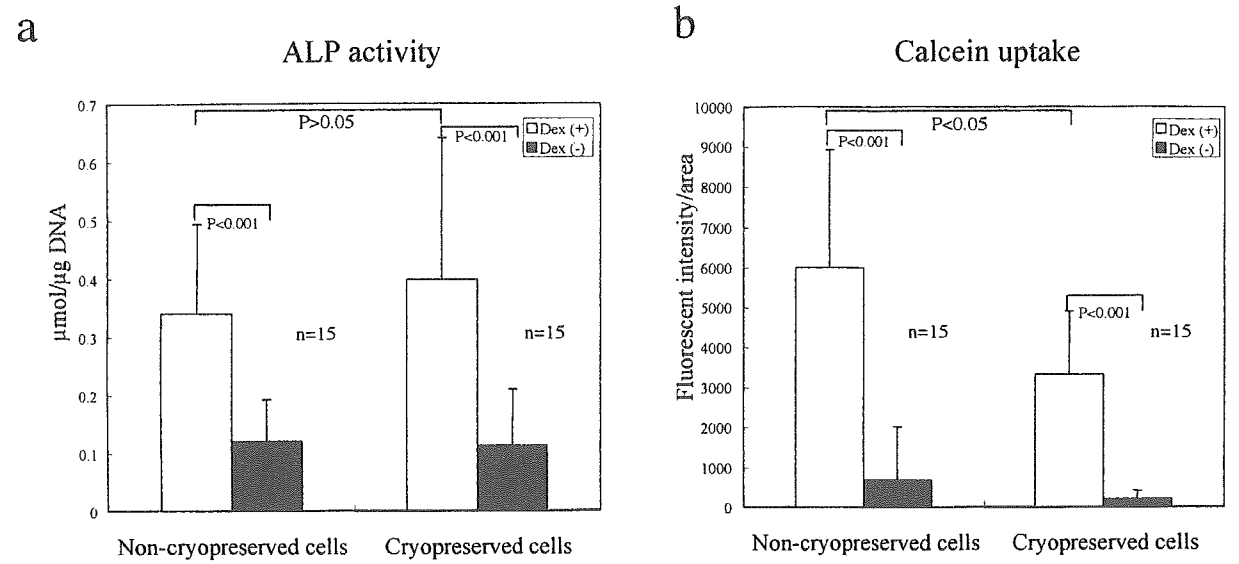

FIG. 3. Osteogenic activities of noncryopreserved and cryopreserved human mesenchymal cells. Fifteen samples of noncryopreserved cells and 15 corresponding samples of cryopreserved cells (nos. 12, 13, and 16–28) are represented with standard deviations (SD). (**a**) ALP activity (μmol/μg DNA) ($p = 0.448$); (**b**) calcein uptake (fluorescence intensity) ($p = 0.004$). Open columns indicate the data of cells cultured in the presence of Dex; solid columns indicate the data of cells cultured in the absence of Dex. Data for the two groups, that is, culturing in the presence or absence of Dex, were examined at a level of significance of $p < 0.001$.

and the biochemical parameters of cryopreserved mesenchymal cells from 15 corresponding cases were measured quantitatively. As for both ALP activity and calcium deposition, both types of mesenchymal cells showed Dex-dependent differentiation. A significant difference between noncryopreserved and cryopreserved cells was not seen in the case of ALP activity ($p > 0.05$). This result indicates that cryopreservation has no influence on the ability of mesenchymal cells to undergo osteoblastic differentiation. However, calcium uptake showed some difference between noncryopreserved and cryopreserved cells ($p < 0.05$).

We analyzed the cell viability of 21 samples (cryopreserved from 0.3 to 37 months) immediately after thawing (Fig. 4). The average cell viability was about 90% (range, 71.9–100%). Application of a straight line to this scatter resulted in $y = -0.0081x + 90.405$, and $R^2 = 0.0002$. These results show that mesenchymal cells can maintain viability in spite of long-term storage.

As shown in Fig. 5, we compared the osteogenic activities (ALP activity and calcein uptake) of 16 samples stored for less than 6 months (defined as short-term) with those of 6 samples stored for 33 to 37 months (defined as long-term). Both groups of mesenchymal cells differentiated Dex dependently, but no significant difference between noncryopreserved and cryopreserved cells was seen ($p > 0.05$). These results show that not only short-term but also long-term cryopreserved mesenchymal cells could maintain their capabilities for osteogenic differentiation.

DISCUSSION

With the rapid advancements in tissue engineering, a multitude of applications for cultured cells in construction of regenerative cultured tissues has been discovered.[3,33] Cultured cells have been used for cell-based therapy and fabrication of tissue-engineered devices. In this regard, we have already been involved in more than 30 cases of human mesenchymal cells from donors to fabricate *in vitro*-cultured regenerative bone for the treatment of various skeletal diseases including arthritis, bone tumors, and osteonecrosis. The cultured mesenchymal cells used for cell-based therapy were all autologous cultured cells without cryopreservation. Some cases, such as arthritis of both the left and right sides, required duplicate treatments with mesenchymal cells and some cases required multiple harvests of fresh bone marrow to expand the number of mesenchymal cells. Therefore, cryopreserved mesenchymal cells that retain a high degree of viability and osteogenic activities, equal to that of primary cultured mesenchymal cells, could be used for such subjects, thus avoiding the risk and possible damage caused by multiple marrow harvests. Furthermore, early bone marrow collection may be highly effective because it is also described that young bone marrow contains more mesenchymal cells than that harvested from older patients.[34] Thus, mesenchymal cells harvested from young patients could be cryopreserved like a "cell bank" with high proliferation and differentiation capabilities and

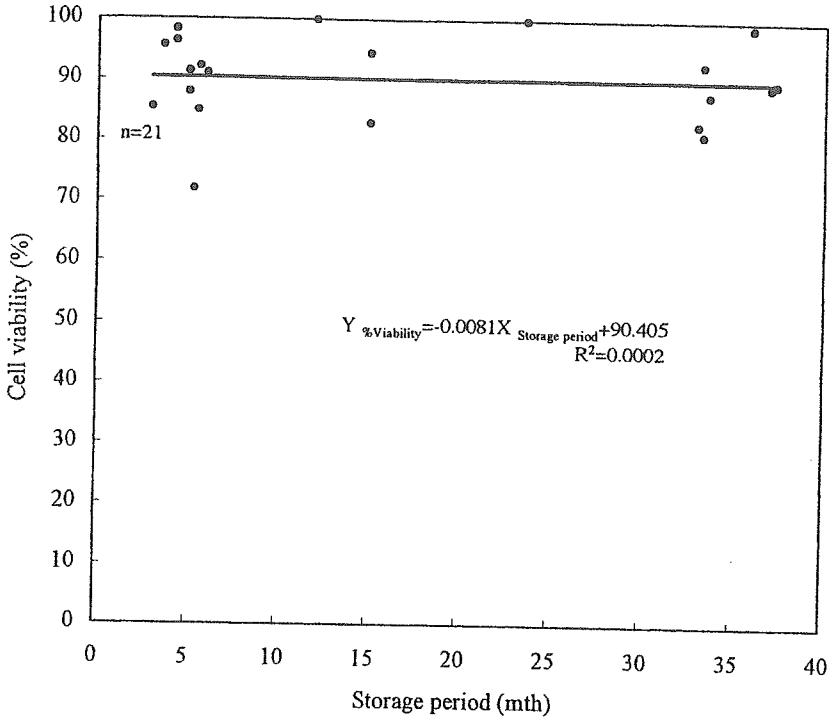

FIG. 4. Viability of cryopreserved human mesenchymal cells relative to storage period. Twenty-one samples of cryopreserved human mesenchymal cells derived from samples 1–11, 15, and 20–28 (see Table 1) were used for determination of cell viability. Immediately after thawing of the cells, cell viability was evaluated with a NucleoCounter. The approximate curve is $y = -0.0081x + 90.405$. $R^2 = 0.0002$. The correlation coefficient is -0.0141.

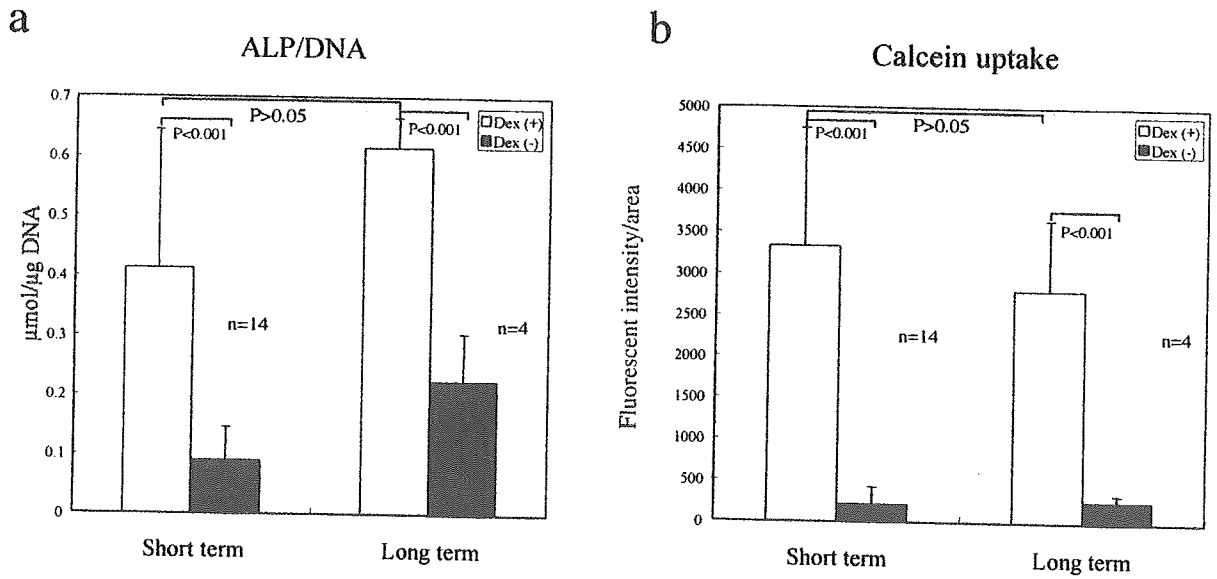

FIG. 5. Osteogenic potential of short-term and long-term cryopreserved human mesenchymal cells. Sixteen samples of short-term cryopreserved cells (nos. 12 and 14–28) and 6 samples (nos. 1–6) of long-term cryopreserved cells are represented. (**a**) ALP activity (μmol/μg DNA) ($p = 0.129$); (**b**) calcein uptake (fluorescence intensity) ($p = 0.185$). Open columns indicate the data of cells cultured in the presence of Dex; solid columns indicate the data of cells cultured in the absence of Dex. The highest and lowest values were not counted by rejection test and the error bars show the standard deviation (SD). Data of the two groups, that is, cultured in the presence or absence of Dex, were examined at a level of significance of $p < 0.001$.

used for future treatment of the same individual. Therefore, if cryopreserved mesenchymal cells were managed at a cell bank, it would be easy to supply numerous MSCs should such be needed.

In this report, we demonstrated the viability of cryopreserved mesenchymal cells. After storage for more than 3 years, cryopreserved cells had a surprisingly high degree of viability, (about 90%), indicating that long-term cryopreservation for several months is not a critical problem. This durability may reflect the nature of the stem cells used in our MSC preparation. Most of these living cells attached to culture-grade dishes in a manner similar to primary cultured cells. The attached cells proliferated well and showed a high degree of osteogenic activity, comparable to that of primary cultured cells. We believed that the calcium deposition level of cryopreserved cells would be similar to that of noncryopreserved cells because cryopreserved cells show the same level of ALP activity compared with noncryopreserved cells (Fig. 3). The amount of calcium deposition derived from cryopreserved cells may be supplemented by additional cultivation. Although the data indicated individual differences in cell viability and osteogenic activities, long-term cryopreservation did not seriously affect these aspects. The results clearly showed that cryopreserved mesenchymal cells could be stored and maintain high degrees of viability and osteogenic potential. Furthermore, the cryopreserved cells were morphologically, phenotypically, and functionally comparable to primary cultured mesenchymal cells. In conclusion, we believe that cryopreserved mesenchymal cells could become a promising candidate cell source for the fabrication of regenerative bone tissues available for a wide range of solutions to bone/joint problems.

Cryopreservation of tissue and cells is a technique that has been utilized by scientists since the 1700s. This process puts the cells in suspended animation, a state in which they can retain their viability indefinitely. In the mid-1900s, the science of cryobiology improved rapidly with the discovery of the beneficial effects of cryoprotectant substances added to cell-freezing solutions. Cryopreservation is now routinely used to store semen, embryos, and all types of cells/tissues from animals and humans. Before freezing, the cells must be treated with a cryoprotectant solution (DMSO or glycerol). These substances protect the cells and their membranes from damage during the freezing process. On the other hand, it has been reported that DMSO is not only cytotoxic but also induces neuron-like cells[35] or cardiac myocytes[36] when added to culture medium. Some groups use a nontoxic cryoprotectant solution such as trehalose in place of DMSO for the cryopreservation of stem cell.[37] In this study, we used DMSO as a cryoprotectant solution and we confirmed that thawed mesenchymal cells had, on average, 90% viability and did not show DMSO-dependent differentiation after cryopreservation (data not shown). But it is surely important to take other cryoprotectant solutions into consideration, because mesenchymal cell must be kept safely for clinical use.

Although it is still difficult to control the differentiation of MSCs with any humoral factors, it has currently been reported that MSCs have multipotentiality as evidenced by their ability to differentiate into numerous cell types such as cardiac myoblasts,[10] vascular endothelial cells,[11,12] hepatocytes,[13] and neural cells.[14] Our current, ongoing study has demonstrated cardiac/vascular regeneration and hepatocyte differentiation using cryopreserved human mesenchymal cells. This study together with other data, clearly demonstrate the excellent viability and differentiative ability of cryopreserved human mesenchymal cells. Consequently, cryopreserved mesenchymal cells may also be applied in the field of regenerative medicine for liver, heart, and vascular regeneration as an MSC source.

ACKNOWLEDGMENTS

This work was supported by the Three-Dimensional Tissue Module Project of METI (a Millennium Project) and a Grant-in-Aid for Scientific Research. We thank Dr. Mitsuo Oshimura (Division of Molecular Genetics and Biofunction, Tottori University) for valuable discussion.

REFERENCES

1. Maniatopoulos, C., Sodek, J., and Melcher, A.H. Bone formation *in vitro* by stromal cells obtained from bone marrow of young adult rat. Cell Tissue Res. **254,** 317, 1988.
2. Le Douarin, N.M., Houssaint, E., Jotereau, F.V., and Belo, M. Origin of hemopoietic stem cells in embryonic bursa of Fabricius and bone marrow studied through interspecific chimeras. Proc. Natl. Acad. Sci. U.S.A. **72,** 2701, 1975.
3. Caplan, A.I., and Bruder, S.P. Mesenchymal stem cells: Building blocks for molecular medicine in the 21st century. Trends Mol. Med. **7,** 259, 2001.
4. Ohgushi, H., Okumura, M., Tamai, S., Shors, E.C., and Caplan, A.I. Marrow cell induced osteogenesis in porous hydroxyapatite and tricalcium phosphate. J. Biomed. Mater. Res. **24,** 1563, 1990.
5. Ohgushi, H., Dohi, Y., Tamai, S., and Tabata, S. Osteogenic differentiation of marrow stromal stem cells in porous hydroxyapatite ceramics. J. Biomed. Mater. Res. **27,** 1401, 1993.
6. Ohgushi, H., Yoshikawa, T., Nakajima, H., Tamai, S., Dohi, Y., and Okunaga, K. Al_2O_3 doped apatite-wollastonite containing glass ceramic provokes osteogenic differentiation of marrow stromal stem cells. J. Biomed. Mat. Res. **44,** 381, 1999.
7. Ohgushi, H., and Caplan, A.I. Stem cell technology and bioceramics: From cell to gene engineering. J. Biomed. Mater. Res. **48,** 913, 1999.

8. Kitamura, S., Ohgushi, H., Hirose, M., Funaoka, H., Takakura, Y., and Ito, H. Osteogenic differentiation of human bone marrow-derived mesenchymal cells cultured on alumina ceramics. Artif. Organs **28,** 72, 2004.
9. Ohgushi, H., Ikeuchi, M., Tateishi, T., Tohma, Y., Tanaka, T., and Takakura, T. Marrow mesenchymal stem cells cultured on alumina ceramics (from basic science to clinical application). Key Eng. Mater. **240,** 651, 2003.
10. Makino, S., Fukuda, K., Miyoshi, S., Konisho, F., Kodama, H., Pan, J., Sano, M., Takahashi, T., Hori, S., Abe, H., Hata, J., Umezawa, A., and Ogawa, S. Cardiomyocytes can be generated from marrow stromal cells *in vitro*. J. Clin. Invest. **103,** 697, 1999.
11. Reyes, M., Dudek, A., Jahagirdar, B., Koodie, L., Marker, P.H., and Verfaillie, C.M. Origin of endothelial progenitors in human postnatal bone marrow. J. Clin. Invest. **109,** 337, 2002.
12. Akahane, M., Ohgushi, H., Kuriyama, S., Akahane, T., and Takakura, Y. Hydroxyapatite ceramics as a carrier of gene-transduced bone marrow cells. J. Orthop. Sci. **7,** 677, 2002.
13. Schwartz, R.E., Reyes, M., Koodie, L., Jiang, Y., Blackstad, M., Lund, T., Lenvik, T., Johnson, S., Hu, W.S., and Verfaillie, C.M. Multipotent adult progenitor cells from bone marrow differentiate into functional hepatocyte-like cells. J. Clin. Invest. **109,** 1291, 2002.
14. Deng, W., Obrocka, M., Fischer, I., and Prockop, D.J. *In vitro* differentiation of human marrow stromal cells into early progenitors of neural cells by conditions that increase intracellular cyclic AMP. Biochem. Biophys. Res. Commun. **282,** 48, 2000.
15. Pittenger, M.F., Mackay, A.M., Beck, S.C., Jaiswal, R.K., Douglas, R., Mosca, J.D., Moorman, M.A., Simonetti, D.W., Craig, S., and Marshak, D.R. Multilineage potential of adult human mesenchymal stem cells. Science **284,** 143, 1999.
16. Jiang, Y., Jahagirdar, B.N., Reinhardt, R.L., Schwartz, R.E., Keene, C.D., Ortiz-Gonzalez, X.R., Reyes, M., Lenvik, T., Lund, T., Blackstad, M., Du, J., Aldrich, S., Lisberg, A., Low, W.C., Largaespada, D.A., and Verfaillie, C.M. Pluripotency of mesenchymal stem cells derived from adult marrow. Nature **418,** 41, 2002.
17. Spurr, E.E., Wiggins, N.E., Marsden, K.A., Lowenthal, R.M., and Ragg, S.J. Cryopreserved human haematopoietic stem cells retain engraftment potential after extended (5–14 years) cryostorage. Cryobiology **44,** 210, 2002.
18. Bruder, S.P., Jaiswal, N., and Haynesworth, E. Growth kinetics, self-renewal, and the osteogenic potential of purified human mesenchymal stem cells during extensive subcultivation and following cryopreservation. J. Cell. Biochem. **64,** 278, 1997.
19. Hirose, M., Kotobuki, N., Machida, H., Kitamura, S., Ohgushi, H., and Tateishi, T. Osteogenic potential of cryopreserved human bone marrow-derived mesenchymal cells after thawing in culture. Mater. Sci. Eng. C **24,** 355, 2004.
20. Kotobuki, N., Hirose, M., Takakura, Y., and Ohgushi, H. Autologous cultured human cells for hard tissue regeneration: Preparation and characterization of mesenchymal stem cells from bone marrow. Artif. Organs **28,** 33, 2004.
21. Reddi, A.H., and Sullivan, N.E. Matrix-induced endochondral bone differentiation: Influence of hypophysectomy, growth hormone, and thyroid-stimulating hormone. Endocrinology **107,** 1291, 1980.
22. Ikeuchi, M., Dohi, Y., Horiuchi, K., Ohgushi, H., Noshi, T., Yoshikawa, T., Yamamoto, K., and Sugimura, M. Recombinant human bone morphogenetic protein-2 promotes osteogenesis within atelopeptide type I collagen solution by combination with rat cultured marrow cells. J. Biomed. Mater. Res. **60,** 61, 2002.
23. Uchimura, E., Machida, H., Kotobuki, N., Kihara, T., Kitamura, S., Ikeuchi, M., Hirose, M., Miyake, J., and Ohgushi, H. *In situ* visualization and quantification of mineralization process of cultured osteogenetic cell. Calcif. Tissue Int. **73,** 575, 2003.
24. Hirose, M., Kotobuki, N., Machida, H., Uchimura, E., and Ohgushi, H. Quantitative monitoring of *in vitro* mineralization process using fluorescent dyes. Key Eng. Mater. **240,** 715, 2003.
25. Young, I.T. Proof without prejudice: Use of the Kolmogorov–Smirnov test for the analysis of histograms from flow systems and other sources. J. Histochem. Cytochem. **25,** 935, 1977.
26. Reyes, M., Lund, T., Lenvik, T., Aguiar, D., Koodie, L., and Verfaillie, C.M. Purification and *ex vivo* expansion of postnatal human marrow mesodermal progenitor cells. Blood **98,** 2615, 2001.
27. Colter, D.C., Sekiya, I., and Prockop, D.J. Identification of a subpopulation of rapidly self-renewing and multipotential adult stem cells in colonies of human marrow stromal cells. Proc. Natl. Acad. Sci. U.S.A. **98,** 7841, 2001.
28. Bianco, P., Riminucci, M., Gronthos, S., and Robey, P.G. Bone marrow stromal stem cells: Nature, biology, and potential applications. Stem Cells **19,** 180, 2001.
29. Majumdar, M.K., Thiede, M.A., Haynesworth, S.E., Bruder, S.P., and Gerson, S.L. Human marrow-derived mesenchymal stem cells (MSCs) express hematopoietic cytokines and support long-term hematopoiesis when differentiated toward stromal and osteogenic lineages. J. Hematother. Stem Cell Res. **9,** 841, 2000.
30. Mosca, J.D., Hendricks, J.K., Buyaner, D., Davis-Sproul, J., Chuang, L.C., Majumdar, M.K., Chopra, R., Barry, F., Murphy, M., Thiede, M.A., Junker, U., Rigg, R.J., Forestell, S.P., Bohnlein, E., Storb, R., and Sandmaier, B.M. Mesenchymal stem cells as vehicles for gene delivery. Clin. Orthop. **379,** 71, 2000.
31. Cheng, L., Qasba, P., Vanguri, P., and Thiede, M.A. Human mesenchymal stem cells support megakaryocyte and pro-platelet formation from $CD34^+$ hematopoietic progenitor cells. J. Cell. Physiol. **184,** 58, 2000.
32. Majumdar, M.K., Thiede, M.A., Mosca, J.D., Moorman, M., and Gerson, S.L. Phenotypic and functional comparison of cultures of marrow-derived mesenchymal stem cells (MSCs) and stromal cells. J. Cell. Physiol. **176,** 57, 1998.
33. Caplan, A.I., Reuben, D., and Haynesworth, S.E. Cell-based tissue engineering therapies: The influence of whole body physiology. Adv. Drug Deliv. Rev. **33,** 3, 1998.
34. Caplan, A.I. Mesenchymal stem cells. J. Orthop. Res. **9,** 641, 1991.
35. Chu, Q., Wang, Y., Fu, X., and Zhang, S. Mechanism of *in vitro* differentiation of bone marrow stromal cells into

neuron-like cells. J. Huazhong Univ. Sci. Technol. Med. Sci. **24,** 259, 2004.
36. Young, D.A., Gavrilov, S., Pennington, C.J., Nuttall, R.K., Edwards, D.R., Kitsis, R.N., and Clark, I.M. Expression of metalloproteinases and inhibitors in the differentiation of P19CL6 cells into cardiac myocytes. Biochem. Biophys. Res. Commun. **24,** 759, 2004.
37. Buchanan, S.S., Gross, S.A., Acker, J.P., Toner, M., Carpenter, J.F., and Pyatt, D.W. Cryopreservation of stem cells using trehalose: Evaluation of the method using a human hematopoietic cell line. Stem Cells Dev. **13,** 295, 2004.

Address reprint requests to:
Hajime Ohgushi, M.D.
Research Institute for Cell Engineering
National Institute of Advanced Industrial Science and Technology
3-11-46 Nakoji
Amagasaki, Hyogo 661-0974, Japan

E-mail: hajime-ohgushi@aist.go.jp

ARTICLE IN PRESS

Available online at www.sciencedirect.com

SCIENCE DIRECT

ELSEVIER

Biochemical and Biophysical Research Communications 341 (2006) 573–582

BBRC

www.elsevier.com/locate/ybbrc

Bioengineered cardiac cell sheet grafts have intrinsic angiogenic potential

Sachiko Sekiya, Tatsuya Shimizu, Masayuki Yamato, Akihiko Kikuchi, Teruo Okano *

Institute of Advanced Biomedical Engineering and Science, Tokyo Women's Medical University, 8-1 Kawada-cho, Shinjuku-ku, Tokyo 162-8666, Japan

Received 16 December 2005

Abstract

Previously, we have demonstrated the long-term survival of myocardial cell sheet constructs in vivo, with microvascular network formation throughout the engineered tissues. The understanding and control of these vascularization processes are a key factor for creating thicker functional tissues. Here, we show that cardiac cell sheets express angiogenesis-related genes and form endothelial cell networks in culture. After non-invasive harvest and stacking of cell sheets using temperature-responsive culture dishes, these endothelial cell networks are maintained and result in neovascularization upon in vivo transplantation. Interestingly, we also discovered that all of the graft vessels are derived from the grafts themselves and these vessels migrate to connect with the host vasculature. Finally, blood vessel formation within the grafts can be controlled by changing the ratio of endothelial cells. In conclusion, myocardial tissue grafts engineered with cell sheet technology have their own inherent potential for the in vivo neovascularization that can be regulated in vitro.

Keywords: Angiogenesis; Vascularization; Myocardial tissue graft; Tissue engineering; Cell sheet

Blood capillaries are precisely organized throughout nearly all tissues and support normal organ function via the supply of nutrients, as well as the removal of various metabolic wastes. In particular, the heart with its high metabolic activity has an increased need for nutrient supplementation and thus possesses an abundant vascular network. Capillary formation within these tissues occurs via two basic vessel-constructing processes: vasculogenesis that occurs in the developing embryo, and angiogenesis, which is the formation of new capillaries via sprouting or intussusception from pre-existing vessels [1].

Vasculogenesis occurs when the primary vascular plexus begins to form primitive blood vessels from angioblasts, which are the embryonic precursors of vascular endothelial cells [2]. After vasculogenesis occurs during embryonic development, new blood vessels are formed via angiogenesis. During the initiation of microvessel formation, there is a focal reduction both between interacting cells, as well as with the surrounding extracellular matrix (ECM), after which, deviation of pericytes occurs and endothelial cells begin to proliferate and migrate in either a sprouting manner or via intussusception. Finally, after the formation of endothelial cell networks via intussusception and cell sprouting, functional blood vessels are constructed by the processes of maturation and remodeling.

In contrast to embryonic vessel development, angiogenesis in adults is generally limited to wound healing and changes in female reproductive organs during the menstrual cycle and pregnancy. However, improper vascularization does occur in some pathological situations, such as ocular neovascularization, inflammatory diseases, and tumor formation [3]. Conversely, critical vascular regression can also cause defects in functional organs, such as myocardial infarction and the formation of pressure sores. Therefore, the development of techniques for the proper regulation of vascularization is of significant clinical interest [4,5].

Recently, regenerative medicine has become increasingly popular as a possible method for treating patients suffering from severe organ failure [6–8]. Ideally, via the combination of biotechnology and cell biology, functional tissues that resemble native structures can be created to replace damaged organs [9–11]. Yet, thus far a major obstacle has been the inability to maintain thick, viable tissues both

* Corresponding author. Fax: +81 3 3359 6046.
E-mail address: tokano@abmes.twmu.ac.jp (T. Okano).

0006-291X/$ - see front matter © 2006 Elsevier Inc. All rights reserved.
doi:10.1016/j.bbrc.2005.12.217

in vitro and in vivo, due to the lack of functional vascular network formation within the engineered constructs [12]. Therefore, it has become increasingly necessary to fabricate functional microvessels within engineered tissues, allowing for the proper supply of nutrients as well as, the removal of waste products, in order to avoid the core ischemia that is observed when tissue thickness is increased. However, while the steps involved in the normal development of blood vessels are well understood, the analogous mechanisms within engineered tissues remain unclear, and thus unable to be either controlled or manipulated. By clarifying these mechanisms of engineered tissue vascularization, approaches to create thicker tissues via the controlled development and manipulation of blood vessels may overcome one of the longstanding obstacles in tissue regeneration therapies.

Previously, we have demonstrated a novel method for tissue regeneration of cell sheet engineering, which uses temperature-responsive culture dishes [13]. With this technology, various types of cultured cells [14–18] can be non-invasively harvested as intact sheets via simple temperature reduction, without the need for proteolytic enzymes [19]. Therefore, vital cell-to-cell interactions that have been previously formed in culture can be maintained even during cell harvest [20]. When cardiac cell sheets were non-invasively harvested and layered in vitro, these three-dimensional constructs showed synchronous pulsations [21]. Upon subcutaneous transplantation of these bioengineered tissues, we also observed the in vivo formation of microvascular networks throughout the entire constructs, allowing for the long-term survival of the pulsatile tissues [21].

In the present study, we demonstrate the first step towards engineering vascularized tissues by elucidating the mechanisms of vessel reconstruction within these myocardial grafts created using cell sheet technology. Finally, after determining the processes involved in graft neovascularization, we show that by regulating endothelial cells within cell sheets, we can control the in vivo neovascularization.

Methods

All procedures using animals in this study were performed in accordance with the "Guide for the Care and Use of Laboratory Animals" (NIH Publication No. 85-23, revised 1996) published by National Institutes of Health, USA, and the "Guidelines of Tokyo Women's Medical University on Animal Use."

Temperature-responsive culture dishes. Specific procedures for the preparation of square-patterned temperature-responsive culture dishes (provided by CellSeed, Tokyo, Japan) have been previously described [22]. Briefly, *N*-isopropylacrylamide (IPAAm) monomer solution was spread onto commercial tissue culture polystyrene dishes. These dishes were then subjected to electron beam irradiation, resulting in polymerization and covalent bonding of IPAAm to the dish surface. Poly-IPAAm (PIPAAm)-grafted dishes were rinsed with cold distilled water to remove ungrafted IPAAm. Next, to prepare square-geometry PIPAAm-grafted cell culture dishes, the PIPAAm-grafted surfaces were masked with a square glass coverslip (24 × 24 mm, Matsunami, Osaka, Japan) and acrylamide (AAm) monomer (Wako Pure Chemicals, Tokyo, Japan) solution was spread onto the masked dish surface. The dish surface was then irradiated by electron beam and washed in the same manner. The resulting culture dishes thus had center square areas grafted with temperature-responsive PIPAAm with a surrounding border grafted with non-cell-adhesive poly-AAm. Culture dishes were finally sterilized by ethylene oxide gas.

Primary culture of neonatal rat cardiac cells. Ventricles from 1-day-old Wister rats (Nisseizai, Tokyo, Japan) were digested at 37 °C in Hanks' solution (Sigma, St. Louis, MO) containing collagenase (class II, Worthington Biochemical, Lakewood, NJ). Isolated cells were suspended in the culture medium comprising 6% FBS (Moregate Biotech, Bulimba, QLD, Australia), 35% Medium 199 (Invitrogen, Carisbad, CA, USA), 71.4 U/ml penicillin-solution, 71.4 μg/ml streptomycin-solution (Sigma, St. Louis, MO), 2.9 mM glucose, and 54% balanced salt solution containing 116 mM NaCl, 1.0 mM NaH_2PO_4, 0.8 mM $MgSO_4$, 1.2 mM KCl, 0.8 mM $CaCl_2$, and 26.2 mM $NaHCO_3$. Cell suspensions were plated at a density of 4.8×10^6 cells per square-geometry PIPAAm-grafted dish and incubated at 37 °C in a humidified atmosphere with 5% CO_2. For enhanced green fluorescent protein (EGFP)-positive cardiomyocytes, ventricles were isolated from EGFP-positive Sprague–Dawley (SD) neonatal rats [SD TgN (act-EGFP) OsbCZ-004], which were kindly provided by Prof. Masaru Okabe (Genome Information Research Center, Osaka University). For 2-methoxyestradiol (2-ME) or vascular endothelial growth factor (VEGF)-treated cells, after 1 day, the culture medium was replaced with fresh media containing either 2 μM 2-ME (Sigma, St. Louis, MO) or 10 nM VEGF (R&D Systems, Minneapolis, MN).

Immunocytochemistry. For endothelial cell staining, myocardial cell sheets were washed with Dulbecco's phosphate-buffered saline (PBS) and then fixed with 4% paraformaldehyde in PBS for 5 min at room temperature. Cells were washed again, blocked with 0.1% normal goat serum, and then incubated with a 1/200 dilution of anti-CD31 monoclonal antibody (Serotec, Oxford, UK) for 1 h at room temperature. A 1/200 dilution of anti-mouse IgG antibody conjugated with Alexa Fluor 488 (Invitrogen, Carlsbad, CA, USA) was applied for 1 h at room temperature as secondary antibody. Cell sheets were finally counterstained with Hoechst 33342 (Wako Pure Chemicals, Tokyo, Japan) for 5 min to visualize cell nuclei. Images were photographed by a AxioCam color digital camera (Carl Zeiss, Hallbergmoss, Germany) using fluorescence microscopy (ECLIPSE TE2000-U, Nikon, Tokyo, Japan) and processed with AxioVision 4.1 software. To quantify endothelial cell network formation, 1300 × 1030 pixel resolution images of cultured cell sheets were captured with a magnification of 40× or 100×. The area of CD31-positive cells in the sheets was calculated with NIH Image software. Data represent the average values of 20 or 5 images in each sample, respectively.

Gene expression analysis. mRNA expression of the angiogenesis-related genes, VEGF, cyclooxygenase (Cox)-2, tyrosine kinase with Ig and EGF homology domains (Tie)-2, Angiopoietin (Ang)-1, and Ang-2 within cardiomyocyte sheets was examined by RT-PCR analysis. Briefly, total RNA of the myocardial cell sheets cultured for either 3 or 7 days was isolated and purified using the RNeasy mini kit (Qiagen, Chatsworth, CA, USA). Reverse transcription was performed with the superscript II RT-PCR system (Invitrogen, Carlsbad, CA, USA) and subsequent PCR was performed with the MPCR Kit for Rat (Maxim Biotech, San Francisco, USA). PCR products were then electrophoresed on 4 % acrylamide gels and stained with ethidium bromide.

Manipulation of cell sheets into layered constructs. Neonatal rat myocardial cells were cultured for 4 days at 37 °C on square-designed temperature-responsive dishes. The culture dishes were set in another CO_2 incubator set at 20 °C to release confluent cells as contiguous cell sheets without enzyme treatments. Cardiomyocyte sheets detached spontaneously within 1 h and became slightly shrunken to about 1 cm^2 cell sheets due to cytoskeletal reorganization and sheet lateral traction forces. The entire cell sheet with media was gently aspirated into the tip of a pipette and the first sheet was transferred again onto a new temperature-responsive dish, with fresh media dropped onto the sheet to spread folded portions. After sheet spreading, media was aspirated and the dish was incubated at 37 °C to allow the cell sheet to fully adhere to the culture surface. To layer cell sheets, another cardiomyocyte sheet detached from a

PIPAAm-grafted dish was transferred and stacked onto the first cell sheet in the same fashion. An identical procedure was repeated to create triple-layer constructs in vitro.

Myocardial graft transplantation into dorsal subcutaneous tissues. EGFP-positive or negative male SD transgenic rats (4–5-weeks-old) or nude rats (4 weeks-old) were anesthetized with intraperitoneal injection of pentbarbital sodium (39 mg/kg). An L-shaped incision (approximately 3 cm × 2 cm) was made in the dorsal skin and lifting of the incised skin exposed the underlying tissue. Triple-layer cardiomyocyte sheets stacked on PIPAAm-grafted surfaces were detached again by lowering the culture temperature and washed with media. The cell constructs were lifted on top of a sterile polypropylene support sheet and transplanted onto dorsal subcutaneous tissues by sliding from the non-adhesive polypropylene sheet. The transplants were covered with 0.5-mm thick silicone membranes (Unique Medical, Tokyo, Japan) to prevent adhesion to the skin and the incisions were closed with 5-0 nylon sutures.

Histological analysis. At appropriate periods after transplantation, myocardial tissue grafts were excised and fixed in 10% neutral buffered formalin (Wako). Tissue specimens were then embedded in paraffin and sliced into 5 μm-thick sections. For hematoxylin and eosin staining, sections were processed by conventional methods. To detect GFP-expressing cells, cross-sections were immunolabeled with a 1/200 dilution of anti-GFP antibody (Invitrogen) for 16 h at 4 °C and secondary stained for 2 h with a 1/400 dilution FITC-conjugated anti-rabbit IgG antibody (Wako) for green fluorescence or Alexa Fluor 568-conjugated anti-rabbit IgG antibody (Invitrogen) for red fluorescence. To detect cardiomyocytes, cross-sections were immunolabeled with a 1/200 dilution of anti-α-sarcomeric actinin (Sigma) for 16 h at 4 °C and secondary stained for 2 h with Alexa Fluor 488-conjugated anti-mouse IgG antibody for green fluorescence or Alexa Fluor 568-conjugated anti-mouse IgG antibodies for red fluorescence. Vessel quantification was examined by counting the number of vessels per unit area, using hematoxylin and eosin stained sections.

Separation of endothelial cells from primary isolated cardiac cells. To regulate the ratio of endothelial cells in the myocardial cell sheets, endothelial cells were separated from primary myocardial cell suspensions by magnetic cell sorting (MACS). Briefly, primary myocardial cell suspensions were incubated with mouse monoclonal anti-rat CD31 antibody. After rinsing with running buffer (PBS containing 5% BSA and 2 mM EDTA), cells were incubated with anti-mouse IgG-conjugated microbeads (Miltenyi Biotec GmbH, Bergisch Gladbach, Germany) and then washed again with running buffer. The labeled cells were applied to the LS column in the magnetic fields of a MiniMACS system (Miltenyi Biotec GmbH, Bergisch Gladbach, Germany). The column was then washed with running buffer and removed from the magnetic fields, and cells trapped in the column were flushed out with running buffer. Endothelial cell-depleted cardiomyocyte suspensions were used to create cell sheets without endothelial cells. To fabricate myocardial cell sheets containing GFP-positive endothelial cells, GFP-negative cardiac cells (without endothelial cells), and purified GFP-positive endothelial cells were mixed in a ratio of 9:1.

Data analysis. All data are expressed as means ± SD. An unpaired Student's *t* test was performed to compare two groups. One-way ANOVA was used for multiple group comparison. If the *F* distribution was significant, a Tukey test was used to specify differences between groups. A *p*-value of less than 0.05 was considered significant.

Results

Angiogenic potential of cardiac cell sheets

To determine whether cardiac cell sheets possess innate potential for vessel formation, the presence of endothelial cells and the expression of angiogenesis-related genes of the cultured cell sheets were examined. Detection of the endothelial cell marker CD31 demonstrated that the pulsatile cardiac cell sheets contained significant amounts of endothelial cells and that the endothelial cells were arranged in a network-like formation after 4 days in culture (Fig. 1A). Gene expression analyses also showed that both VEGF and cyclooxygenase-2 (Cox-2), which are well-known angiogenesis-accelerating genes, were expressed continuously in the cultured cell sheets, in vitro (Fig. 1B). Significant mRNA expression of Tie-2, an endothelial cell-specific receptor, was also detected within the cardiac cell sheets (Fig. 1B). Correspondingly, Ang-1, a ligand of Tie-2, which is involved in the maturation process of blood vessel formation, was occasionally expressed, while Ang-2, which antagonizes Ang-1 binding to Tie-2, could not be detected (Fig. 1C). Taken together, these results indicate that the pulsatile cardiac cell sheets possessed their own potential for neovascularization, with the presence of endothelial cells in a network-like arrangement and the expression of major genes related to the promotion of vessel formation.

Endothelial cell network formation in cardiac cell sheets

To further examine the endothelial networks that were present within the cardiac cell sheets, the presence of CD31-positive cells was monitored throughout the culture period. One day after cell seeding, cardiomyocytes within the cell sheets began to pulsate asynchronously, but only a low number of sparsely distributed endothelial cells could be observed (Fig. 2A). At two days, the cells within the cardiac sheets began to beat synchronously and endothelial cells begin to proliferate and sprout within the sheets (Fig. 2B). Three days after initial cell seeding, the sprouting endothelial cells began to connect to each other (Fig. 2C) and at 4 days, these sprouting endothelial cells formed cell networks throughout the cardiomyocyte sheets (Fig. 2D). Quantification of the CD31-positive area within the cell sheets also showed that the area correlated to endothelial cells increased over time and accounted for 11.7 ± 5.9% of the total cell sheet area at 4 days (Fig. 2E). Additionally, these endothelial cell networks within the cardiac cell sheets were similar in appearance to the well-known sprouting form of endothelial cells cultured in Matri-gel. Finally, we also observed the occasional tubulogenesis of endothelial cells within the cardiac cell sheets, however these detected tubular structures had no continuity in vitro (data not shown).

To examine the reactivity of endothelial cells in cardiac cell sheets, cultured cells were treated with either 2-ME or VEGF, to examine their effects on network formation. In comparison to untreated controls, which showed an average of 8.0 ± 0.2% CD31-positive areas (Fig. 3A), after treatment with 2-ME, endothelial cell network formation was significantly diminished, representing only 0.3 ± 0.2% of the total area (Fig. 3B). In contrast, the addition of VEGF to the culture medium promoted endothelial cell network formation (13.6 ± 5.2%) (Fig. 3C), demonstrating that the cardiac cell sheets contained actively formed endothelial cell networks, having the characteristic nature of native blood vessels.

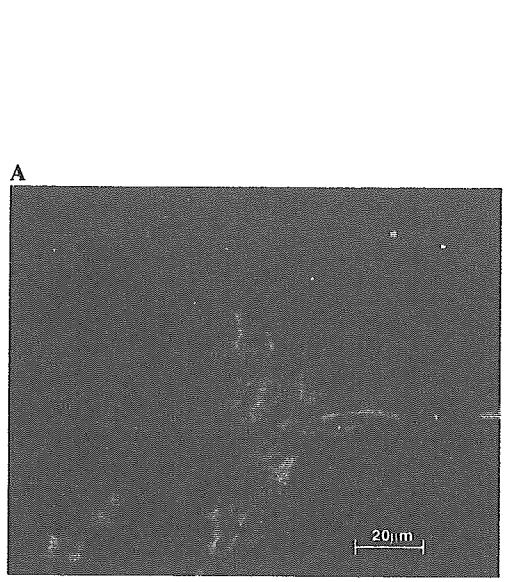

C

Gene	Result
VEGF	++
Cox-2	++
Tie-2	++
Ang-1	+
Ang-2	-

Fig. 1. Cardiac cell sheets have intrinsic angiogenic potential. (A) Endothelial cells within cardiac cell sheets were detected as CD31-expressing cells (green). Nuclei (blue) are counterstained with Hoechst 33342. (B) RT-PCR analysis of RNA isolated from cardiac cell sheets shows positive expression for VEGF, Cox-2, and Tie-2 at both 3 and 7 days in culture. (C) Total gene expression analysis of angiogenesis-related genes detected in cardiac cell sheets by RT-PCR. (++) indicates expression, (+) indicates occasional expression, and (−) indicates no expression.

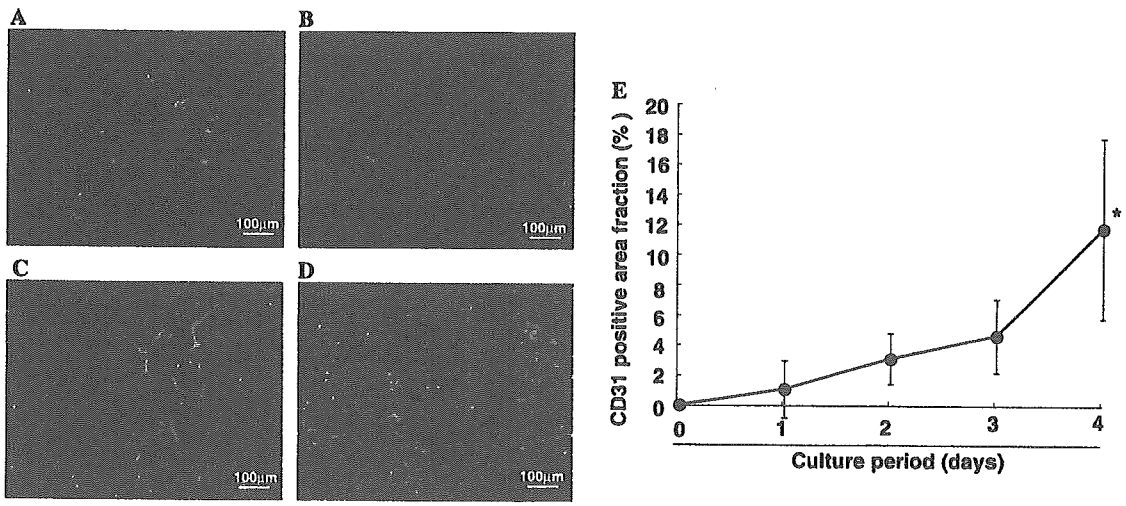

Fig. 2. Endothelial cells within cardiac cell sheets grow in a sprouting fashion. CD31 expression within the cardiac cell sheets was detected at (A) 1 day, (B) 2 days, (C) 3 days, and (D) 4 days, in culture. (E) The graph shows the percentage of CD31-positive areas of the myocardial cell sheets at each time period. ($*p < 0.05$, $n = 3$).

Neovascularization of myocardial tissue grafts occurs upon in vivo transplantation

To determine the origin of newly formed blood vessels within the myocardial tissue grafts in vivo, we stacked three cardiac cell sheets derived from EGFP-expressing neonatal rats and transplanted these triple-layer grafts into the dorsal subcutaneous tissues of normal rats. When the transplantation sites were opened 1 week after the procedures, the implanted grafts showed synchronous and spontaneous pulsation and maintained their original shapes, indicating whole tissue survival. Upon histological analysis

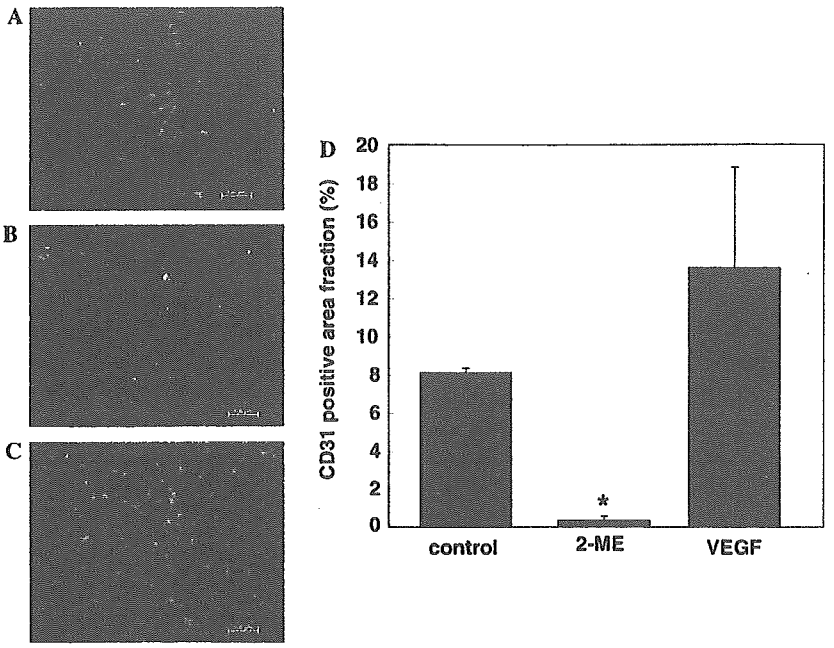

Fig. 3. Endothelial cells within cardiac cell sheets are reactive. Immunostaining for CD31 in (A) control, (B) cells treated with 2 μM 2-methoxyestradiol or (C) 10 nM rat recombinant VEGF shows changes in endothelial cell network formation after 4 days in culture. (D) The graph shows the percentage of CD31-positive areas of the myocardial cell sheets treated under each condition ($*p < 0.05$, $n = 3$).

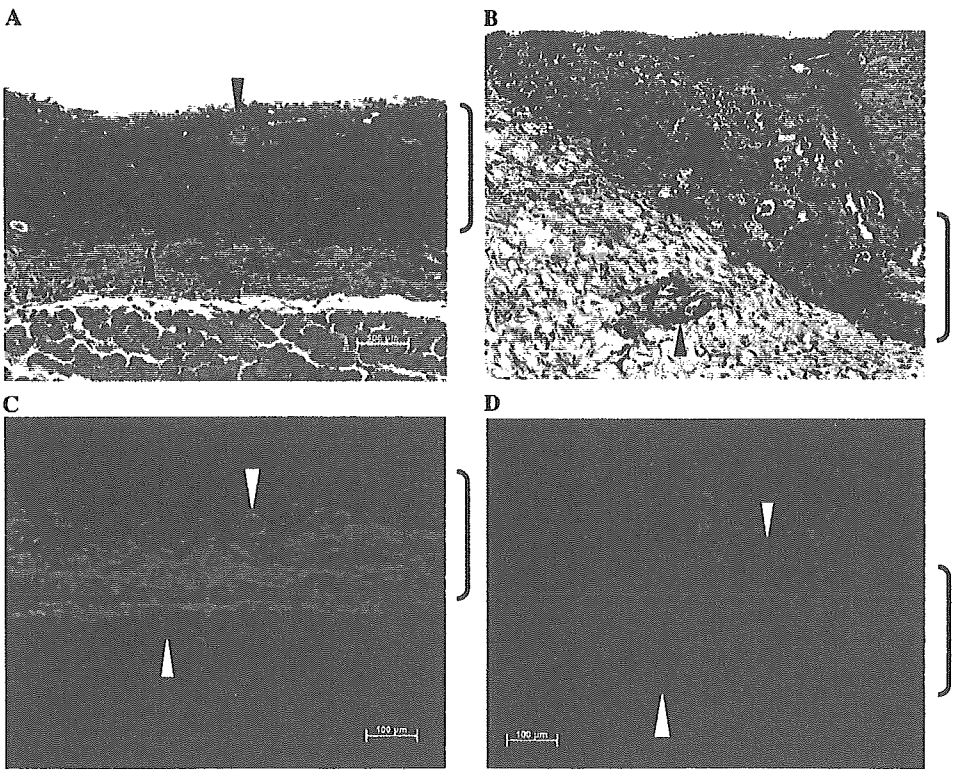

Fig. 4. Microvessel formation within transplanted triple-layer cardiac cell sheets. One week after transplantation, (A,B) show hematoxylin and eosin staining which shows the formation of microvessels containing host erythrocytes within the transplanted grafts and in the underlying host tissues (black arrowheads). (C,D) Anti-EGFP immunostaining (red fluorescence) identifies graft-derived cells. Arrows indicate that the vessels observed in (A,B) are EGFP-positive and contain host erythrocytes within the lumen of the vessels (white arrowheads). Note that EGFP-positive vessels sprout into the host tissue.

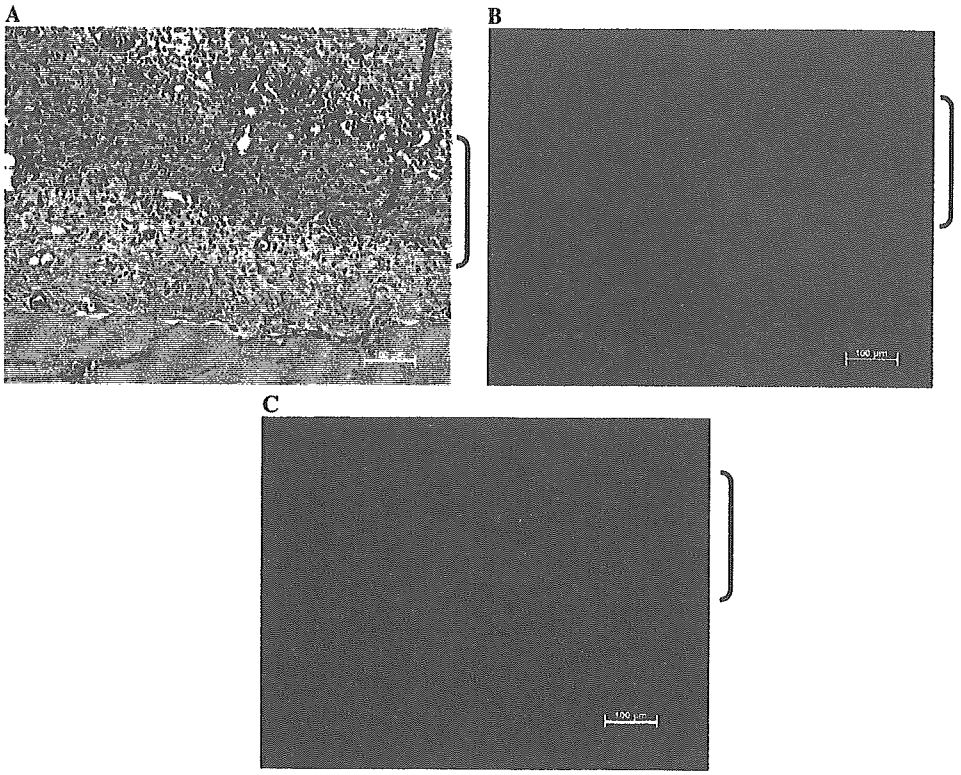

Fig. 5. Immunohistological analysis of the myocardial tissue grafts transplanted subcutaneously into EGFP-expressing host rats. One week after transplantation, (A) hematoxylin and eosin staining demonstrates microvessel formation within the EGFP-negative transplanted tissues. (B) Immunostaining for EGFP (red) shows almost no positive staining within the transplanted grafts, indicating that the vessel formation is due to EGFP-negative graft cells. (C) anti-α-sarcomeric actinin demonstrates the presence of cardiac muscle in the transplanted grafts.

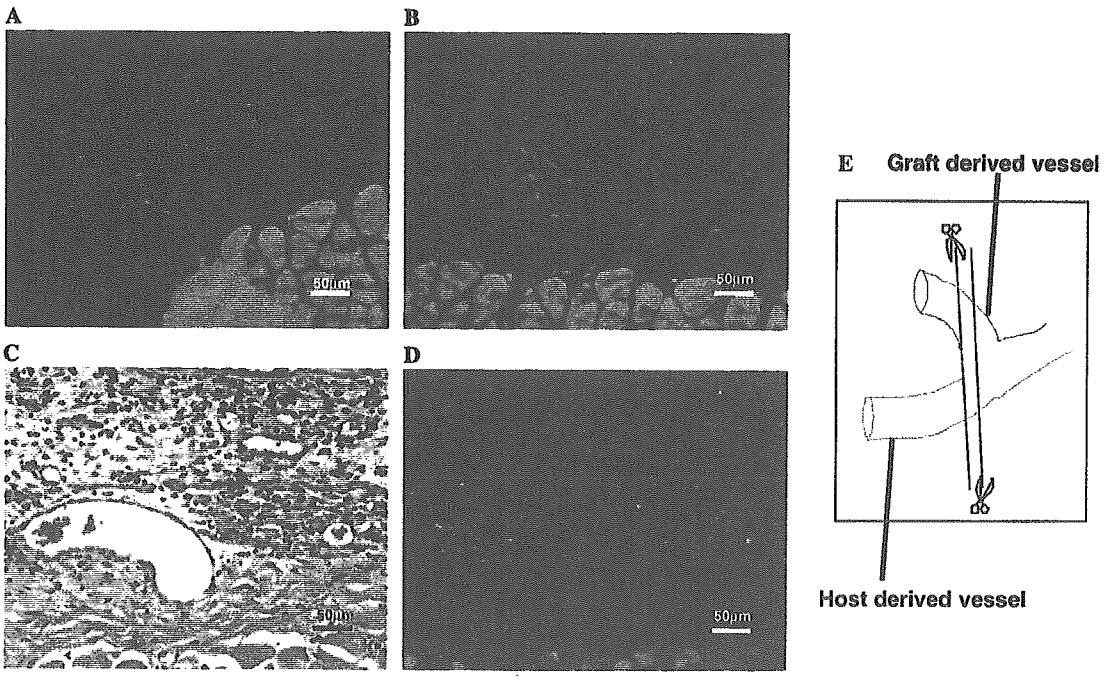

Fig. 6. Fused vessels at the junction between the EGFP-expressing host tissues and the transplanted grafts. (A,B) Immunostaining EGFP (green) demonstrates that EGFP-negative graft endothelial cells fuse with EGFP-positive host cells to form mature microvessels. (C) Hematoxylin and eosin staining of a serial section to (A,B) shows erythrocytes within the vessel lumen. (D) Immunostaining for α-sarcomeric actinin (green) shows that the vessel is at the border between the transplanted cardiac grafts and the underlying host tissues. (E) Presents a schematic illustration of the observed serial sections.

of resected tissues, well-established vascular structures within the grafts were observed, similar to our previously reported results [21] (Figs. 4A and B). Unexpectedly however, anti-GFP antibody staining clearly demonstrated that almost all blood vessels in the grafts expressed EGFP and were therefore graft-derived (Figs. 4C and D). Furthermore, some EGFP-expressing blood vessels, originating from the transplanted grafts, could even be detected within the host tissues just beneath the implanted cardiac tissues (Figs. 4C and D).

To determine whether host-derived vessels migrated into the transplanted cardiac grafts, EGFP-negative myocardial tissue grafts were transplanted into EGFP-expressing host rats. One week after transplantation, no EGFP-positive blood vessels could be detected within the myocardial tissue grafts (Figs. 5A and B), which were positively stained for cardiac muscle, by anti-α-sarcomeric actinin antibody (Fig. 5C). Using staining of serial cross-sections, it was also observed that EGFP-positive host vessels fused with EGFP-negative graft vessels at the border region between the transplanted myocardial grafts and the underlying host subcutaneous tissues (Fig. 6). These results therefore indicated that endothelial cell networks within the cell sheets mature to form tubularized vascular networks within the grafts after in vivo transplantation. Additionally, these newly formed vessels that originated completely from the grafts migrated into the underlying tissues to connect with host blood vessels.

Controlling neovascularization within myocardial tissue grafts

Due to the observation that the newly formed vessels within the implanted myocardial tissues were completely graft-derived, we tried to control the ratio of endothelial cells within the fabricated cardiac cell sheets and exam-

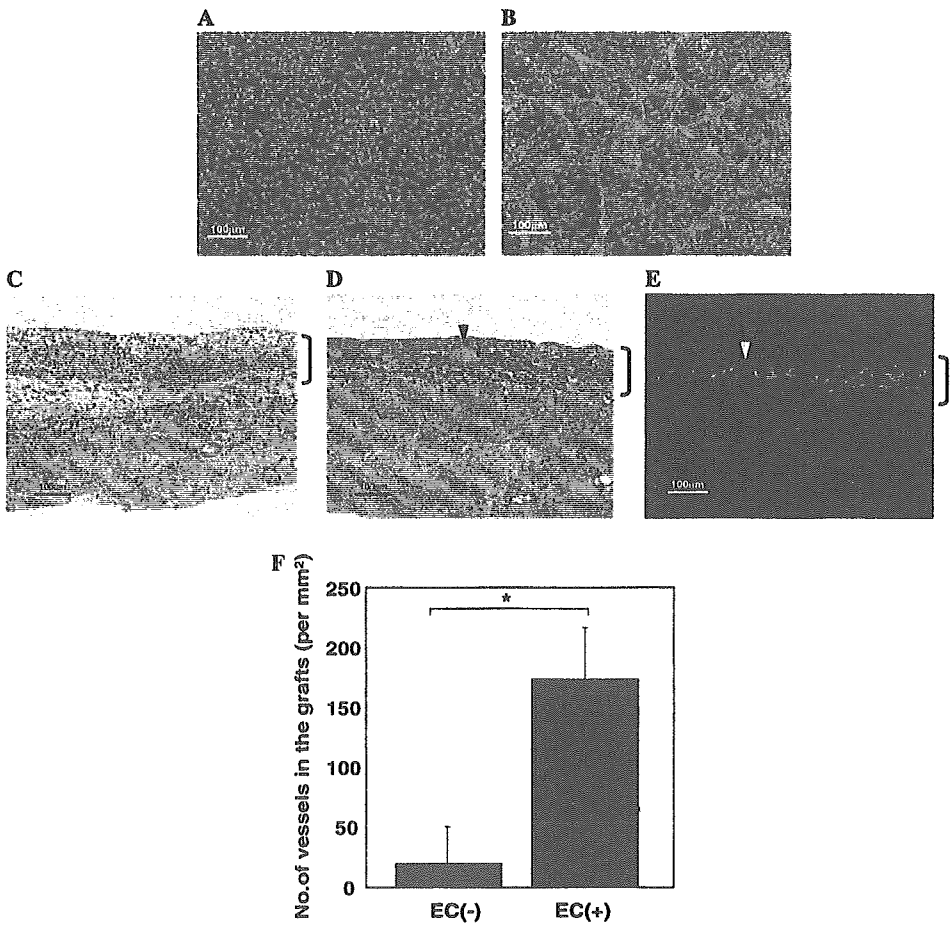

Fig. 7. Control of endothelial cells allows for the regulation of in vivo neovascularization. Endothelial cells were removed from isolated cardiac cell suspensions by MACS. (A) Anti-CD31 staining shows that cardiac cell suspensions without endothelial cells do not form sprouting endothelial cell networks in vitro. (B) When endothelial cells were added to cardiac cells at a ratio of 1:9, in vitro sprouting network formation could be recovered. (C) Three days after triple-layer subcutaneous transplantation, cardiac cell sheets with no endothelial cells demonstrate no vessel formation in vivo. (D) In contrast, when EGFP-positive endothelial cells were added at a ratio of 1:9, in vivo blood vessel formation was also recovered. (E) Anti-EGFP immunostaining demonstrates that all the blood vessels within the grafts are derived from graft-originating EGFP-positive cells (green). (F) Quantitative analysis of vessel formation within the fabricated grafts is presented. EC (−) indicates the grafts fabricated without endothelial cells and EC (+) created with endothelial cells and cardiac cells at a ratio of 1:9. (*$p < 0.05$, $n = 3$).

ined the effect on graft neovascularization in vivo. Endothelial cells were separated from primary isolated cardiac cell suspensions by MACS and accounted for $18.9 \pm 9.8\%$ ($n = 7$) of the total isolated cell suspensions. When cardiac cell sheets without endothelial cells were fabricated from the remaining cell suspensions after MACS, significantly fewer endothelial networks were observed (Fig. 7A). However, when endothelial cell-depleted cardiac cells were mixed with EGFP-positive endothelial cells at a ratio of 9:1, the previously observed endothelial cell networks could be completely recovered within these hybrid cell sheets (Fig. 7B). Upon subcutaneous transplantation of triple-layer mixed cell sheets into nude rats, graft-originated EGFP-positive blood vessels were clearly observed within the transplanted myocardial tissue grafts (Figs. 7D and E). When transplanted grafts were composed of cell sheets without endothelial cells, a significantly lower amount of blood vessels were observed 3 days after implantation (Fig. 7C), compared to the hybrid cell sheet group that contained a controlled ratio of endothelial cells. These findings therefore confirmed that the endothelial cells within the cell sheet grafts contribute significantly to the formation of new blood vessels within the bioengineered tissues (Fig. 7F). Moreover, by controlling the ratio of endothelial cells initially seeded in the cardiac cell sheets, neovascularization of the fabricated grafts could also be regulated.

Discussion

There have been several previous studies regarding micro blood vessel formation of tissue implants without surgical vascular anastomoses. When human skin grafts were transplanted onto athymic mice, graft vessels became anastomosed to the host circulation, but over time, human endothelial cells from the transplanted grafts progressively degenerate while host endothelial cells invade to gradually replace the graft-derived cells [23]. Similarly, in the case of pancreatic islet grafts transplanted both subcutaneously and to the kidney capsule, the transplanted tissues were shown to be mainly re-vascularized by endothelial cells of host origin [24,25]. Additionally, when cultured skin substitutes were transplanted into rat subcutaneous tissues, new blood vessel formation was shown to be due to both graft- and host-derived endothelial cells [26].

In contrast to these previously reported results, when we transplanted triple-layer cardiac cell sheet constructs into dorsal subcutaneous tissues, the observed blood vessel reconstruction was completely due to the endothelial cell networks that originated from within the grafts. Interestingly, these newly formed graft-derived blood vessels also sprouted into the underlying host tissues, to form functional connections with the host vasculature. Furthermore, vasculature regulation experiments in vivo also demonstrated that the endothelial cell network in vitro forms functional microvessels and sprout into the host tissues after transplantation.

Many biological factors, such as ECM molecules and secreted proteins, have been shown to be important for endothelial cell network formation in engineered tissues [27]. It is well known that when endothelial cells are cultured in three-dimensional Matri-gel and collagen-based gels, they undergo a reversible transition from a resting cobblestone formation to a sprouting angiogenic phenotype [28,29]. Similarly, when endothelial cells were included in the cardiac cell sheets, they showed this sprouting form and network development in vitro, even though additional ECM substitutes were not used. With our method, the isolated cell suspensions include not only cardiomyocytes and endothelial cells, but also a significant number of fibroblasts and other ECM-producing cells. Therefore, it is likely that these cells can produce the appropriate ECM molecules such as collagen, which can act to promote endothelial network formation within the cardiac cell sheets.

In combination with the ECM environment, various secreted proteins, such as growth factors and cytokines, have also been shown to be involved in the neovascularization processes. In our results, mRNA expression of both VEGF and Cox-2 was observed, in vitro within the cardiac cell sheets. It has been reported that VEGF secretion via cardiomyocytes is required for the development of coronary microvessels [30], and VEGF gene expression of cultured cardiomyocytes has been also previously demonstrated [31]. Cox-2 is also a key enzyme involved in angiogenesis and known to be expressed in cardiomyocytes [32]. Furthermore, when human umbilical vein endothelial cells were cultured with conditioned medium derived from rat neonatal cardiomyocytes, Cox-2 expression was also induced in the endothelial cells by VEGF secreted by the cardiac cells [33], indicating that VEGF production by cardiomyocytes within the cell sheets, and Cox-2 expression, may accelerate endothelial sprouting and network formation. Likewise, direct cell-to-cell interactions between cardiomyocytes and endothelial cells have been reported to rescue cardiomyocytes from undergoing apoptosis in vitro, with these effects enhanced compared to the use of conditioned media [34]. Previously, the co-culture of endothelial cells, fibroblasts, and skeletal myoblasts, within three-dimensional porous scaffolds, has also shown to play a significant role in the vascularization of engineered skeletal muscle [27], demonstrating the importance of cell-to-cell interactions in creating endothelial cell networks. In cardiac cell sheets, the observation that cardiomyocyte clusters surround areas enriched with endothelial cells also suggests that the endothelial cell networks are activated by both direct cell-to-cell interactions, as well as secreted proteins from cardiomyocytes. Therefore, a mutually beneficial relationship between cardiomyocytes and endothelial cells seems to contribute to the formation of endothelial cell networks in vitro.

A key factor in the ability for the rapid neovascularization of the bioengineered grafts in vivo is the use of cell sheet engineering with temperature-responsive culture dishes, which are created by the covalent grafting of the

temperature-responsive polymer, PIPAAm, onto ordinary tissue culture polystyrene (TCPS) surfaces [13,19]. With traditional cell harvest methods using proteolytic enzymes such as trypsin, cells are collected as single or isolated cell suspensions. In such cases, it can be expected that the endothelial networks that have been formed, as well as crucial cell-to-cell interactions between cardiomyocytes and endothelial cells, would be disrupted. With temperature-responsive dishes, cells can be cultured on these surfaces similarly onto normal TCPS surfaces at 37 °C. However, by simply reducing the culture temperature to 20 °C, the dish surfaces undergo a reversible transition from hydrophobic to hydrophilic. When this occurs, the grafted polymer rapidly swells, such that a hydration layer is formed between the dish surface and the cultured cells, allowing for all the cultured cells along with their deposited ECM to be non-invasively harvested as intact sheets [20]. Therefore, with cardiac cell sheets harvested from temperature-responsive dishes, their own deposited ECM is preserved, and the cell sheets are also able to retain intact, undisrupted endothelial cell networks, as well as the expression of angiogenesis-accelerating genes such as VEGF and Cox-2. The ability to maintain the differentiated state that has developed during culture is in stark contrast to cell harvest with proteolytic enzymes and allows for the rapid development of graft-derived endothelial cell networks into mature microvessels upon transplantation of these bioengineered tissues with an innate ability for vascularization.

For future applications of tissue engineering, and more specifically related to cardiac tissues, the creation of thick, cell-dense constructs with functional vessels is required. Yet at the present time, growth factor administration and gene therapies methods still remain relatively difficult to control both in vitro and in vivo. In the present study however, upon determining the neovascularization mechanisms of myocardial tissue grafts, we clearly demonstrate the possibility of controlling in vivo vascularization by regulating the ratio of endothelial cells in cardiomyocyte sheets. From these results, it is clearly conceivable that by applying the co-culture of different endothelial cell sources and varying the ratio of endothelial cells within the grafts, optimal conditions for blood vessel fabrication within specific tissues can be created.

Similarly, while the formation of endothelial cell networks can be controlled, these immature networks can survive for only 1 week, in vitro (data not shown). Therefore, not only biological factors but also physical stimuli such as flow and shear stress are likely required to mimic the in vivo environment and allow for the formation of mature vascular networks, under in vitro conditions [35,36].

In conclusion, myocardial tissue grafts engineered with cell sheet technology have their own inherent potential for the in vivo reconstruction of blood vessels. By controlling the endothelial cell population within the cardiac cell sheets, the potential for vascularization can also be regulated, which will likely overcome the limits of mass transport to create thick and functional tissues. This engineering of structures that more closely resemble native tissues has the potential for new applications for tissue engineering and regenerative medicine, as well as other areas, by creating more realistic experimental model systems.

Acknowledgments

We appreciate the useful comments and technical criticism from Mr. Joseph Yang (Tokyo Women's Medical University). We also thank Prof. Masaru Okabe (Osaka University) for kindly providing EGFP transgenic rats and Ms. Yuko Kanauchi (Toho University) for helpful assistance with the endothelial cell regulation studies. The present work was supported by grants for the Center of Excellence Program for the 21st Century, the High-Tech Research Center Program and Grant-in Aid for Young Scientists (B) from the Ministry of Education, Culture, Sports, Science and Technology (MEXT); the Research Grants for Cardiovascular Disease and Regenerative Medicine from the Ministry of Health, Labour and Welfare; and the Open Research Grant from the Japanese Research Promotion Society for Cardiovascular Diseases.

References

[1] W. Risau, Mechanisms of angiogenesis, Nature 386 (1997) 671–674.
[2] W. Risau, I. Flamme, Vasculogenesis, Annu. Rev. Cell Dev. Biol. 11 (1995) 73–91.
[3] J. Folkman, Angiogenesis in cancer, vascular, rheumatoid and other disease, Nat. Med. 1 (1995) 27–31.
[4] M. Ueda, Y. Terai, K. Kanda, M. Kanemura, M. Takehara, H. Futakuchi, H. Yamaguchi, M. Yasuda, K. Nishiyama, M. Ueki, Tumor angiogenesis and molecular target therapy in ovarian carcinomas, Hum. Cell 18 (2005) 1–16.
[5] A. Kawamoto, H.C. Gwon, H. Iwaguro, J.I. Yamaguchi, S. Uchida, H. Masuda, M. Silver, H. Ma, M. Kearney, J.M. Isner, T. Asahara, Therapeutic potential of ex vivo expanded endothelial progenitor cells for myocardial ischemia, Circulation 103 (2001) 634–637.
[6] C.J. Koh, A. Atala, Tissue engineering, stem cells, and cloning: opportunities for regenerative medicine, J. Am. Soc. Nephrol. 15 (2004) 1113–1125.
[7] K.M. Kulig, J.P. Vacanti, Hepatic tissue engineering, Transpl. Immunol. 12 (2004) 303–310.
[8] H.M. Nugent, E.R. Edelman, Tissue engineering therapy for cardiovascular disease, Circ. Res. 92 (2003) 1068–1078.
[9] M. Brittberg, A. Lindahl, A. Nilsson, C. Ohlsson, O. Isaksson, L. Peterson, Treatment of deep cartilage defects in the knee with autologous chondrocyte transplantation, N. Engl. J. Med. 331 (1994) 889–895.
[10] R.S. Kirsner, V. Falanga, W.H. Eaglstein, The development of bioengineered skin, Trends Biotechnol. 16 (1998) 246–249.
[11] T. Shin'oka, Y. Imai, Y. Ikada, Transplantation of a tissue-engineered pulmonary artery, N. Engl. J. Med. 344 (2001) 532–533.
[12] T. Walles, T. Herden, A. Haverich, H. Mertsching, Influence of scaffold thickness and scaffold composition on bioartificial graft survival, Biomaterials 24 (2003) 1233–1239.
[13] N. Yamada, T. Okano, H. Sakai, F. Karikusa, Y. Sawasaki, Y. Sakurai, Thermo-responsive polymeric surfaces; control of attachment and detachment of cultured cells, Makromol. Chem. Rapid Commun. 11 (1990) 571–576.
[14] M. Harimoto, M. Yamato, M. Hirose, C. Takahashi, Y. Isoi, A. Kikuchi, T. Okano, Novel approach for achieving double-layered cell sheets co-culture: overlaying endothelial cell sheets onto monolayer

hepatocytes utilizing temperature-responsive culture dishes, J. Biomed. Mater. Res. 62 (2002) 464–470.

[15] K. Nishida, M. Yamato, Y. Hayashida, K. Watanabe, N. Maeda, H. Watanabe, K. Yamamoto, S. Nagai, A. Kikuchi, Y. Tano, T. Okano, Functional bioengineered corneal epithelial sheet grafts from corneal stem cells expanded ex vivo on a temperature-responsive cell culture surface, Transplantation 77 (2004) 379–385.

[16] K. Nishida, M. Yamato, Y. Hayashida, K. Watanabe, K. Yamamoto, E. Adachi, S. Nagai, A. Kikuchi, N. Maeda, H. Watanabe, T. Okano, Y. Tano, Corneal reconstruction with tissue-engineered cell sheets composed of autologous oral mucosal epithelium, N. Engl. J. Med. 351 (2004) 1187–1196.

[17] Y. Shiroyanagi, M. Yamato, Y. Yamazaki, H. Toma, T. Okano, Urothelium regeneration using viable cultured urothelial cell sheets grafted on demucosalized gastric flaps, BJU Int. 93 (2004) 1069–1075.

[18] J. Yang, M. Yamato, C. Kohno, A. Nishimoto, H. Sekine, F. Fukai, T. Okano, Cell sheet engineering: recreating tissues without biodegradable scaffolds, Biomaterials 26 (2005) 6415–6422.

[19] T. Okano, N. Yamada, H. Sakai, Y. Sakurai, A novel recovery system for cultured cells using plasma-treated polystyrene dishes grafted with poly(*N*-isopropylacrylamide), J. Biomed. Mater. Res. 27 (1993) 1243–1251.

[20] A. Kushida, M. Yamato, C. Konno, A. Kikuchi, Y. Sakurai, T. Okano, Decrease in culture temperature releases monolayer endothelial cell sheets together with deposited fibronectin matrix from temperature-responsive culture surfaces, J. Biomed. Mater. Res. 45 (1999) 355–362.

[21] T. Shimizu, M. Yamato, Y. Isoi, T. Akutsu, T. Setomaru, K. Abe, A. Kikuchi, M. Umezu, T. Okano, Fabrication of pulsatile cardiac tissue grafts using a novel 3-dimensional cell sheet manipulation technique and temperature-responsive cell culture surfaces, Circ. Res. 90 (2002) e40–e48.

[22] M. Hirose, O.H. Kwon, M. Yamato, A. Kikuchi, T. Okano, Creation of designed shape cell sheets that are noninvasively harvested and moved onto another surface, Biomacromolecules 1 (2000) 377–381.

[23] M. Demarchez, D.J. Hartmann, M. Prunieras, An immunohistological study of the revascularization process in human skin transplanted onto the nude mouse, Transplantation 43 (1987) 896–903.

[24] T. Linn, K. Schneider, H.P. Hammes, K.T. Preissner, H. Brandhorst, E. Morgenstern, F. Kiefer, R.G. Bretzel, Angiogenic capacity of endothelial cells in islets of Langerhans, FASEB J. 17 (2003) 881–883.

[25] P. Vajkoczy, A.M. Olofsson, H.A. Lehr, R. Leiderer, F. Hammersen, K.E. Arfors, M.D. Menger, Histogenesis and ultrastructure of pancreatic islet graft microvasculature. Evidence for graft revascularization by endothelial cells of host origin, Am. J. Pathol. 146 (1995) 1397–1405.

[26] D.M. Supp, K. Wilson-Landy, S.T. Boyce, Human dermal microvascular endothelial cells form vascular analogs in cultured skin substitutes after grafting to athymic mice, FASEB J. 16 (2002) 797–804.

[27] S. Levenberg, J. Rouwkema, M. Macdonald, E.S. Garfein, D.S. Kohane, D.C. Darland, R. Marini, C.A. van Blitterswijk, R.C. Mulligan, P.A. D'Amore, R. Langer, Engineering vascularized skeletal muscle tissue, Nat. Biotechnol. 23 (2005) 879–884.

[28] S. Kobayashi, E. Ito, R. Honma, Y. Nojima, M. Shibuya, S. Watanabe, Y. Maru, Dynamic regulation of gene expression by the Flt-1 kinase and Matrigel in endothelial tubulogenesis, Genomics 84 (2004) 185–192.

[29] I. Segura, A. Serrano, G.G. De Buitrago, M.A. Gonzalez, J.L. Abad, C. Claveria, L. Gomez, A. Bernad, A.C. Martinez, H.H. Riese, Inhibition of programmed cell death impairs in vitro vascular-like structure formation and reduces in vivo angiogenesis, FASEB J. 16 (2002) 833–841.

[30] F.J. Giordano, H.P. Gerber, S.P. Williams, N. VanBruggen, S. Bunting, P. Ruiz-Lozano, Y. Gu, A.K. Nath, Y. Huang, R. Hickey, N. Dalton, K.L. Peterson, J. Ross Jr., K.R. Chien, N. Ferrara, A cardiac myocyte vascular endothelial growth factor paracrine pathway is required to maintain cardiac function, Proc. Natl. Acad. Sci. USA 98 (2001) 5780–5785.

[31] A.P. Levy, N.S. Levy, J. Loscalzo, A. Calderone, N. Takahashi, K.T. Yeo, G. Koren, W.S. Colucci, M.A. Goldberg, Regulation of vascular endothelial growth factor in cardiac myocytes, Circ. Res. 76 (1995) 758–766.

[32] N. Degousee, J. Martindale, E. Stefanski, M. Cieslak, T.F. Lindsay, J.E. Fish, P.A. Marsden, D.J. Thuerauf, C.C. Glembotski, B.B. Rubin, MAP kinase 6-p38 MAP kinase signaling cascade regulates cyclooxygenase-2 expression in cardiac myocytes in vitro and in vivo, Circ. Res. 92 (2003) 757–764.

[33] G. Wu, A.P. Mannam, J. Wu, S. Kirbis, J.L. Shie, C. Chen, R.J. Laham, F.W. Sellke, J. Li, Hypoxia induces myocyte-dependent COX-2 regulation in endothelial cells: role of VEGF, Am. J. Physiol. Heart Circ. Physiol. 285 (2003) H2420–H2429.

[34] D.A. Narmoneva, R. Vukmirovic, M.E. Davis, R.D. Kamm, R.T. Lee, Endothelial cells promote cardiac myocyte survival and spatial reorganization: implications for cardiac regeneration, Circulation 110 (2004) 962–968.

[35] B.P. Chen, Y.S. Li, Y. Zhao, K.D. Chen, S. Li, J. Lao, S. Yuan, J.Y. Shyy, S. Chien, DNA microarray analysis of gene expression in endothelial cells in response to 24-h shear stress, Physiol. Genomics 7 (2001) 55–63.

[36] J.P. Cullen, S. Sayeed, R.S. Sawai, N.G. Theodorakis, P.A. Cahill, J.V. Sitzmann, E.M. Redmond, Pulsatile flow-induced angiogenesis: role of G(i) subunits, Arterioscler. Thromb. Vasc. Biol. 22 (2002) 1610–1616.

The FASEB Journal express article 10.1096/fj.05-4715fje. Published online January 26, 2006.

Polysurgery of cell sheet grafts overcomes diffusion limits to produce thick, vascularized myocardial tissues

Tatsuya Shimizu,* Hidekazu Sekine,* Joseph Yang,* Yuki Isoi,* Masayuki Yamato,* Akihiko Kikuchi,* Eiji Kobayashi,† and Teruo Okano*

*Institute of Advanced Biomedical Engineering and Science, Tokyo Women's Medical University, 8-1 Kawada-cho, Shinjuku-ku, Tokyo 162-8666; and †Division of Organ Replacement Research, Center for Molecular Medicine, Jichi University Medical School, 3311-1 Minamikawachi-machi, Kawachi-gun, Tochigi 329-0498 Japan

Tatsuya Shimizu and Hidekazu Sekine contributed equally to this work.

Corresponding author: Teruo Okano, Ph.D., Institute of Advanced Biomedical Engineering and Science, Tokyo Women's Medical University 8-1 Kawada-cho, Shinjuku-ku, Tokyo 162-8666 Japan. E-mail: tokano@abmes.twmu.ac.jp

ABSTRACT

Recently, the field of tissue engineering has progressed rapidly, but poor vascularization remains a major obstacle in bioengineering cell-dense tissues, limiting the viable size of constructs due to hypoxia, nutrient insufficiency, and waste accumulation. Therefore, new technologies for fabricating functional tissues with a well-organized vasculature are required. In the present study, neonatal rat cardiomyocytes were harvested as intact sheets from temperature-responsive culture dishes and stacked into cell-dense myocardial tissues. However, the thickness limit for layered cell sheets in subcutaneous tissue was ~80 μm (3 layers). To overcome this limitation, repeated transplantation of triple-layer grafts was performed at 1, 2, or 3 day intervals. The two overlaid grafts completely synchronized and the whole tissues survived without necrosis in the 1 or 2 day interval cases. Multistep transplantation also created ~1 mm thick myocardium with a well-organized microvascular network. Furthermore, functional multilayer grafts fabricated over a surgically connectable artery and vein revealed complete graft perfusion via the vessels and ectopic transplantation of the grafts was successfully performed using direct vessel anastomoses. These cultured cell sheet integration methods overcome long-standing barriers to producing thick, vascularized tissues, revealing a possible solution for the clinical repair of various damaged organs, including the impaired myocardium.

Key words: poly(*N*-isopropylacrylamide) • electrophysiology • microsurgery

Since Langer and Vacanti first reported the formation of bioengineered cartilage tissue shaped as an ear within mouse dorsal subcutaneous tissues, the field of tissue engineering has progressed rapidly. This initial study described constructs fabricated by seeding cell suspensions into three-dimensional (3-D) biodegradable scaffolds molded into the proper size and shape of an ear (1, 2). Since then, many researchers have attempted to reconstruct various tissues

using this scaffold-based technology to restore damaged or lost organ functions (3–7), with tissue-engineered substitutes for skin, cartilage, and large-scale vasculature already clinically applied (8–10). Recently, bioengineered myocardium has been pursued as one of the next generation tissue products due to the large number of patients suffering from severe heart failure (11–15).

Nonetheless, despite these promising developments, new problems now challenge the field. One major barrier regards effective reconstruction of cell-dense tissues, such as the heart, liver, and kidney. In scaffold-based tissue engineering, seeding of isolated cell suspensions into porous polymer scaffolds often fails to produce high cell density and remains problematic. Moreover, such scaffolds are gradually replaced with extracellular matrix (ECM) upon biodegradation, producing cell-sparse tissue engineered constructs with abundant ECM. Hence, scaffold-based tissue engineering appears more useful for ECM-rich tissues, but insufficient for successful reconstruction of cell-dense tissues. A critical, additional obstacle opposing cell-dense tissue fabrication is the inability to constantly and rapidly supply sufficient essential nutrients while removing metabolic wastes via reliable vascular networks. This feature is in contrast to reduced requirements for vascular supply in cell-sparse tissues. The lack of sufficient vascularization induces necrosis in bioengineered tissues, restricting growth and limiting their final mass. New technologies for improving the reconstruction of three-dimensional, cell-dense functional tissues accompanied by a well-organized vascular network are thus also strongly desired.

We have developed an original scaffold-free tissue engineering technology, "cell sheet engineering," to facilitate reconstruction of 3-D tissues by stacking monolayer confluently cultured cell sheets. Cultured cell sheets are harvested from temperature-responsive culture surfaces covalently grafted with the temperature-responsive polymer, poly(*N*-isopropylacrylamide) (PIPAAm) (16, 17). While confluently cultured cells are typically harvested as isolated cell suspensions by enzymatic digestion, confluent cells cultured on PIPAAm-grafted surfaces release as contiguous viable cell sheets simply by lowering the culture temperature (18). Cultured cell sheets are released without any enzymatic digestion due to the rapid surface transition from hydrophobic (cell-adhesive) to hydrophilic (non cell-adhesive), with full preservation of cell-to-cell connections in the cultured monolayer (19). We have already established cell sheet manipulation techniques for various cell types and applied this technology for tissue engineering (20–25). For example, using a single cell sheet method, autologous oral mucosal epithelial cells were used to replace damaged corneal surfaces in early human applications, with visual acuity remarkably recovered in all patients (26). For cell-dense 3-D tissue reconstruction, we have applied cell sheet technology to myocardial tissue engineering (27). In myocardium, electrical and structural cell-to-cell tight junctions are critical to synchronized, functional beating. We have already confirmed both electrical and morphological communication between multiple cultured layered neonatal rat cardiomyocyte sheets as well as used these cell sheets to successfully fabricate simultaneously beating myocardial tissues both in vivo and in vitro (28). Direct contact of layered confluent cell sheets promotes rapid electrical and mechanical synchronization and functional beating of the bioengineered myocardium. From these results, we assert that layered cell sheet technology presents a significant advantage over scaffold-based tissue engineering in fabricating cell-dense functional tissues. However, the lack of proper vascularization still prevents unlimited stacking of additional cell sheets due to mass transport problems.